

N1-Coordination in palladium(II) and platinum(II) complexes with 9-methylhypoxanthine: crystal structures and theoretical calculations†

José Ruiz,^{*a} Natalia Cutillas,^a María Dolores Villa,^a Gregorio López,^a Arturo Espinosa^b and Delia Bautista^c

Received 29th July 2009, Accepted 9th September 2009

First published as an Advance Article on the web 26th September 2009

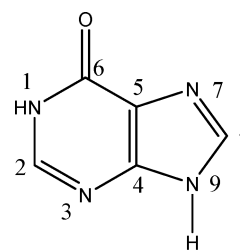
DOI: 10.1039/b915427b

The synthesis of the new palladium and platinum complexes with 9-methylhypoxanthine (9-mhypH) of the type $[M(\text{dmba})(L)(9\text{-mhypH-N}7)]\text{ClO}_4$ [$\text{dmba} = \text{N,C-chelating 2-(dimethylaminomethyl)phenyl}$; $M = \text{Pd or Pt}$; $L = \text{DMSO, PPh}_3$ or PTA ($\text{PTA} = 1,3,5\text{-Triaza-7-phosphaadamantane}$)] is reported. Pd(II) and Pt(II) complexes with the anion of 9-mhypH of the type $[M(\text{dmba})(L)(9\text{-mhyp-N}1)]$ [$L = \text{PPh}_3$ or PTA] have also been prepared. The crystal structures of $[\text{Pt}(\text{dmba})(\text{PPh}_3)(9\text{-mhypH-N}7)]\text{ClO}_4$ and $[\text{Pt}(\text{dmba})(\text{PPh}_3)(9\text{-mhyp-N}1)]$ have been established by X-ray diffraction. The last complex is the first structurally authenticated example of N1 coordination of 9-methylhypoxanthine to platinum. DFT-based calculations at the BP86/def2TZVP level predict a most favourable interaction (both kinetically and thermodynamically) of the metal(II) centre with N7 in the neutral ligand 9-mhypH, but with N1 in the deprotonated ligand 9-mhyp⁻ in agreement with the experimentally observed preference in neutral conditions or upon basic treatment, respectively.

Introduction

The discovery of the anticarcinogenic activity of *cis*- $[\text{PtCl}_2(\text{NH}_3)_2]$ (cisplatin) by B. Rosenberg in 1969 has led to research interests being focused on the interactions of Pt compounds with nucleic acids and their constituents.^{1–3} From a chemical point of view, considerable effort has been paid to the various binding modes.⁴ Selective coordination to a nucleobase is influenced by structural and electronic factors arising from the nucleobase and the complex itself.^{5–9} It is well known that hypoxanthine (Chart 1) is a naturally occurring purine derivative that occasionally can be found as a constituent of nucleic acids where it is present in the anticodon of tRNA in the form of its nucleotide inosine.¹⁰

The synthesis of the antitumor drug cisplatin derivative containing the purine model nucleobase *cis*- $[\text{Pt}(\text{NH}_3)_2(9\text{-madeH-N}6)(9\text{-mhypH-N}7)]^{2+}$ (9-mhypH = 9-methylhypoxanthine, 9-madeH = 9-methyladenine)¹¹ and the cationic tetrakis(nucleobase)¹² complex $[\text{Pt}(9\text{-mhypH-N}7)_4]^{2+}$ has been reported. The compounds *trans*- $[(\text{NH}_3)_2\text{Pt}(9\text{-mhypH-N}7)_2]^{2+}$ and *trans*- $[(\text{CH}_3\text{NH}_2)_2\text{Pt}(1\text{-MeC-N}3)(9\text{-mhypH-N}7)]^{2+}$ (1-MeC = 1-methylcytosine) have also been previously prepared.¹³



Hypoxanthine

Chart 1

In this article we describe the synthesis of mononuclear palladium and platinum complexes of the type $[M(\text{dmba})(L)(9\text{-mhypH-N}7)]\text{ClO}_4$ [$\text{dmba} = \text{N,C-chelating 2-(dimethylaminomethyl)phenyl}$; $M = \text{Pd or Pt}$; $L = \text{DMSO, PPh}_3$ or PTA ($\text{PTA} = 1,3,5\text{-Triaza-7-phosphaadamantane}$)] and $[M(\text{dmba})(L)(9\text{-mhyp-N}1)]$ [$M = \text{Pd or Pt}$; $L = \text{PPh}_3$ or PTA]. $[\text{Pt}(\text{dmba})(\text{PPh}_3)(9\text{-mhyp-N}1)]$ is the first structurally authenticated example of N1 coordination of 9-methylhypoxanthine according to a search of the Cambridge Structure Database (CSD).¹⁴ The experimentally observed preference for the coordination to the metal(II) centre using the N7 atom as donor in neutral conditions and N1 upon basic treatment has been studied by means of computational calculations.

Results and discussion

Complexes $[M(\text{dmba})(L)(9\text{-mhypH})]\text{ClO}_4$

The dmba complexes 1–4 have been prepared from the corresponding chlorometal complex $[M(\text{dmba})(L)\text{Cl}]$ ($M = \text{Pd or Pt}$).^{15,16} After precipitation of AgCl by addition of AgClO_4 in a 1:1 molar ratio in acetone, the solvent complexes $[M(\text{dmba})(L)(\text{Me}_2\text{CO})]\text{ClO}_4$ ($M = \text{Pd or Pt}$), generated *in situ*, react with 1 equiv of 9-mhypH

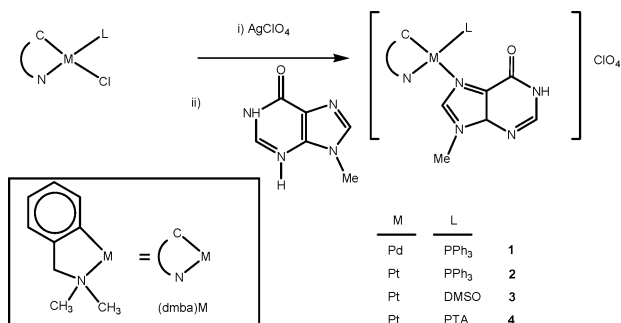
^aDepartamento de Química Inorgánica, Facultad de Química, Universidad de Murcia, 30071, Murcia, Spain. E-mail: jrui@um.es; Fax: +34 868 884148; Tel: +34 868 887455

^bDepartamento de Química Orgánica, Facultad de Química, Universidad de Murcia, 30071, Murcia, Spain. E-mail: artuesp@um.es; Fax: +34 868 884149; Tel: +34 968367489

^cUniversidad de Murcia, SAI, 30071, Murcia, Spain. E-mail: dbc@um.es; Fax: +34 968 367302; Tel: +34 868 88 4165

† Electronic supplementary information (ESI) available: Selected geometrical parameters for experimental and calculated structures of **2** and **6**. Figures with the calculated structures of **2**^{calc} and **6**^{calc}. Cartesian coordinates and energies for all calculated species. HSAB-derived global and group parameters for the reaction of 9-mhypH derivatives with the Pt atom in $[\text{Pt}(\text{PPh}_3)(\text{dmab})]^+$. CCDC reference numbers 742533 & 742534. For ESI and crystallographic data in CIF or other electronic format see DOI: 10.1039/b915427b

to give the cationic complexes $[M(\text{dmba})(L)(9\text{-mhyph})]\text{ClO}_4$ (**1–4**) (Scheme 1). Complexes **1–4** are white, air stable solids that decompose on heating above 200°C in a dynamic N_2 atmosphere. NMR, electrospray ionization (ESI) mass spectrometry, and elemental analysis were used to characterize **1–4**. ESI mass spectra of **1–4** show peaks with a recognisable isotope pattern corresponding to $[\text{Pt}(\text{dmba})(L)(9\text{-mhyph})]^+$ ($L = \text{DMSO}, \text{PPh}_3$ or PTA). Their acetone solutions show conductance values corresponding to 1:1 electrolytes (Λ_M in the range $135\text{--}145 \text{ S cm}^2 \text{ mol}^{-1}$),¹⁷ which indicates the presence of the neutral ligand HmtpO in these complexes. An IR band is observed at *ca.* 1095 which is assigned to the ν_3 mode of free perchlorate (T_d symmetry). The observation of an additional band at *ca.* 623 cm^{-1} for the ν_4 mode confirms the presence of free perchlorate.¹⁸ The IR spectra also show a very strong band at *ca.* 1705 cm^{-1} assigned to the $\nu(\text{CO})$ of the neutral 9-mhyph (1680 cm^{-1} for the free ligand). COSY and NOESY experiments were used for the assignment. The ^1H NMR spectra of complexes **1–4** are consistent with the N^7 metal coordination of the 9-methylhydropoxanthine. Thus H8 exhibits a noe effect with NMe_2 protons of dmbs and H2 shows a noe effect with the NH of 9-mhyph. In complexes **1, 2** and **4** the phosphine-*trans*-to- NMe_2 ligand arrangement in the starting products^{15,16} is preserved, after chlorine abstraction and 9-mhyph coordination, as can be inferred by ^1H NMR from the small, but significant, coupling constant $^4J_{\text{P-H}}$ (2.5 Hz) of the CH_2N or the NMe_2 protons of dmbs with the phosphorus atom.¹⁹ Platinum satellites are observed as shoulders in several of the resonances of complexes **2–4** ($I = 1/2$, natural abundance 33.8). It is also noteworthy that the proton resonance of H2 of the coordinated 9-mhyph of complexes **3** and **4** is duplicated, which could be as a consequence of the slightly different chemical environment of the nucleus caused by two possible orientations in DMF-d_7 solution.



Scheme 1

Crystal structure of 2. The structure of **2** consists of mononuclear $[\text{Pt}(\text{dmbs})(\text{PPh}_3)(9\text{-mhyph-N7})]^+$ cations and perchlorate anions. The cation of **2** is depicted in Fig. 1. The angles around platinum deviate from 90° due to the bite of the cyclometallated ligand, the $\text{C}(1)\text{--Pt}(1)\text{--N}(1)$ angle of $81.46(8)^\circ$ being within the normal range for such complexes.^{9,19} The PPh_3 ligand is *trans* to the nitrogen donor, displaying no tendency to occupy the position *trans* to the σ -bound orthoplatinated aryl group.²⁰ The cyclometallated ring is puckered with the nitrogen atom significantly out of the plane defined by the platinum and carbon atoms, a feature which is quite commonly observed in cyclometallated dmbs complexes.^{7,9,21} In the crystal, the perchlorate anion is

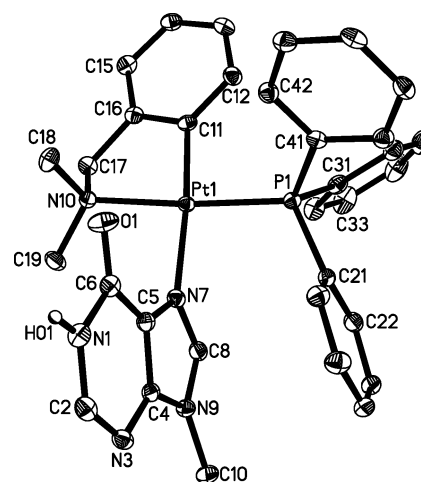


Fig. 1 ORTEP representation (50% probability) of **2**. Selected bond lengths (\AA) and angles (deg): $\text{Pt}(1)\text{--C}(11) = 2.016(2)$, $\text{Pt}(1)\text{--N}(7) = 2.1253(18)$, $\text{Pt}(1)\text{--N}(10) = 2.1390(17)$, $\text{Pt}(1)\text{--P}(1) = 2.2333(5)$, $\text{C}(11)\text{--Pt}(1)\text{--N}(10) = 81.46(8)$, $\text{C}(1)\text{--Pt}(1)\text{--N}(7) = 172.66(7)$, $\text{N}(7)\text{--Pt}(1)\text{--N}(10) = 92.67(7)$, $\text{C}(11)\text{--Pt}(1)\text{--P}(1) = 94.34(6)$, $\text{P}(1)\text{--Pt}(1)\text{--N}(7) = 91.64(5)$, $\text{N}(10)\text{--Pt}(1)\text{--P}(1) = 175.46(5)$.

bridging three complex cations through $\text{N}\text{--H}\cdots\text{O}$ and $\text{C}\text{--H}\cdots\text{O}$ bonds in which the NH, CH_3 , CH_2 and CH groups are involved. Furthermore, there is an intramolecular interaction by phenyl-9-mhyph π -stacking (centroid-centroid distance: 3.487 \AA).²² There is also an intermolecular stacking interaction between 9-mhyph pairs yielding a centrosymmetric dimer arrangement (Fig. 2), and an intermolecular stacking interaction between phenyl pairs is also present (centroid-centroid distance: 3.780 \AA). Intermolecular aromatic CH/π interactions^{9,23–25} are also found.

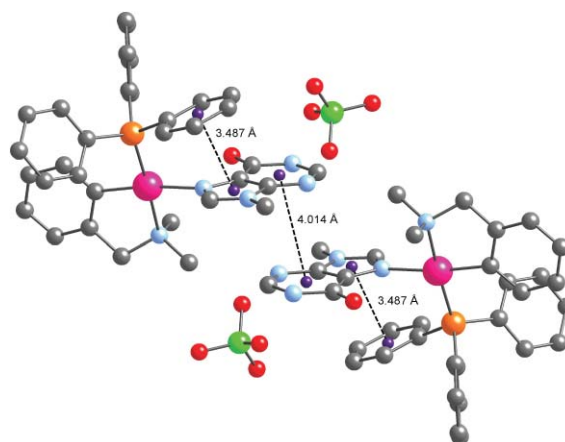
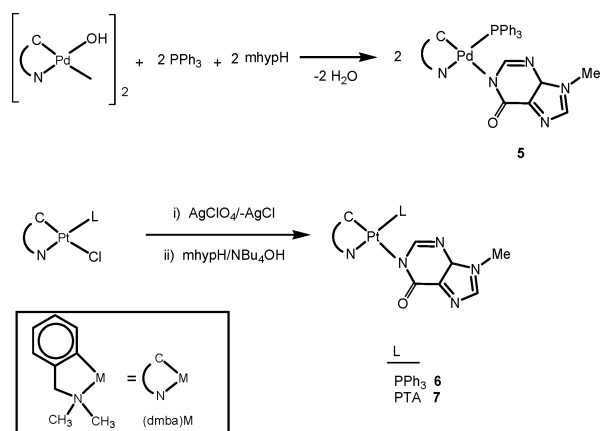


Fig. 2 Relevant π -stacking interactions in complex **2**.

Complexes $[\text{M}(\text{dmbs})(L)(9\text{-mhyph-N1})]$

The reaction in dichloromethane at room temperature of the hydroxopalladium complex $[\text{Pd}(\text{dmbs})(\mu\text{-OH})_2]$ ²⁶ with PPh_3 and 9-mhyph in the molar ratio 1:2:2 leads to the formation of the mononuclear palladium complex $[\text{Pd}(\text{dmbs})(\text{PPh}_3)(9\text{-mhyph-N1})]$ (**5**) (Scheme 2). The platinum analogous complexes have been prepared from the corresponding chloro platinum complex



Scheme 2

[Pt(dmab)(L)Cl] (L = PPh₃ or PTA)¹⁶ (Scheme 2). After precipitation of AgCl by addition of AgClO₄ in a 1:1 molar ratio in acetone, the solvent complexes [Pt(dmab)(L)(Me₂CO)]ClO₄ generated *in situ* react with 1 equiv of both 9-mhyph and [NBu₄]OH to give the neutral complexes [Pt(dmab)(L)(9-mhyph-N1)] (L = PPh₃ or PTA; **6** and **7**).

Complexes **5–7** are white and air-stable solids. Their acetone solutions show no conductance values which indicates the presence of the anionic ligand 9-mhyph in these complexes. The structure was assigned also on the basis of microanalytical, IR and ¹H and ³¹P NMR data. The ν(CO) band of the IR spectra of complexes **5–7** is observed at 1630 cm⁻¹, which is a significant difference when comparing with the values (over 1705 cm⁻¹) observed for complexes **1–4**, containing the neutral 9-mhyph ligand. The ¹H NMR spectra of complexes **5–7** show that both the *N*-methyl and the CH₂ group of the dmab are diastereotopic, two separate signals being observed for the former and an AB quartet for the later (some broadening being observed for complex **5**). Therefore there is no plane of symmetry in the metal coordination plane. The assignment of the H8 and H2 signals in complexes **5–7** was made by NOESY. The inversion in the chemical shifts of these signals compared with the corresponding values observed in complexes **1–4** is in agreement with the literature values of *cis*-[Pt(NH₃)₂(9-mhyph-N1)(9-made-N6)]²⁺, where the N1-coordination of 9-mhyph has been suggested.³ The X-ray crystal structure of complex **6** (*vide infra*) supports this assignment.

Crystal Structure of 6. The structure of **6** is shown in Fig. 3. This is the first structurally authenticated example of N1 coordination of 9-methylhypoxanthine to platinum according to a search of the Cambridge Structure Database (CSD).¹⁴ Thus, in the previously reported²⁷ related complex *trans*-[PtCl(NH₃)₂(9-mhyph)]·2H₂O the metal coordinates to N7 of the 9-mhyph. The packing of complex **6** is stabilized predominantly by hydrogen bonding giving centrosymmetric or head-to-tail dimer arrangements (see the ESI†), the C(6)O group of the nucleobase being also involved (Fig. 4). Intermolecular contacts^{23–25} C–H···π_{9-mhyph} (Fig. 5) and C–H···π_{ph} are also observed. Stacking of the hypoxanthine bases does not seem to play an important role in stabilizing the crystal packing of **6**. It has been suggested that deprotonation of the N1H site leads to an increase in the electron

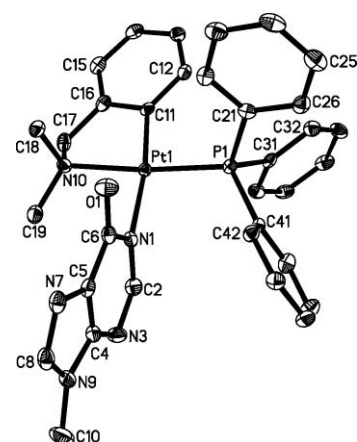


Fig. 3 ORTEP representation (50% probability) of **6**. Selected bond lengths (Å) and angles (deg): Pt(1)–C(11) = 2.017(3), Pt(1)–N(1) = 2.108(3), Pt(1)–N(10) = 2.138(3), Pt(1)–P(1) = 2.2148(9), C(11)–Pt(1)–N(10) = 81.76(13), C(11)–Pt(1)–N(1) = 171.76(13), N(10)–Pt(1)–N(1) = 90.25(11), C(11)–Pt(1)–P(1) = 94.94(11), P(1)–Pt(1)–N(1) = 93.18(8), N(10)–Pt(1)–P(1) = 174.42(8).

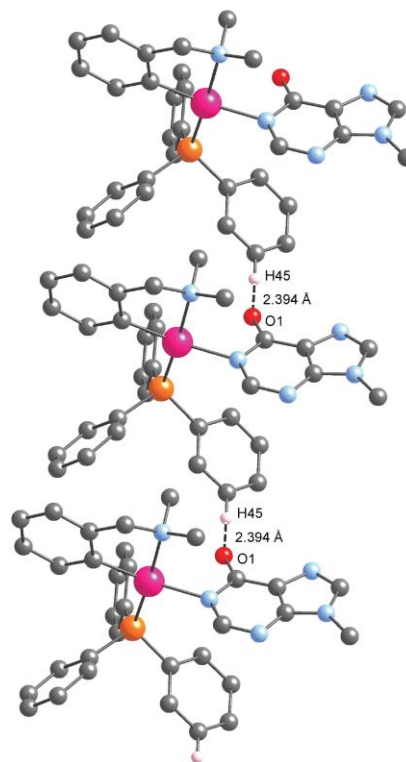


Fig. 4 Intermolecular C–H···O interactions in **6**.

density in the heterocyclic ring and probably causes repulsion between the base moieties.²⁸

Theoretical calculations

Binding of the aforementioned 9-methylhypoxanthine (9-mhyph) to the metallic Pt centre in either neutral or basic media has also been studied by quantum chemical calculations. The experimentally observed preference for the coordination to the metal(II) centre using the N7 atom as donor in neutral conditions and N1

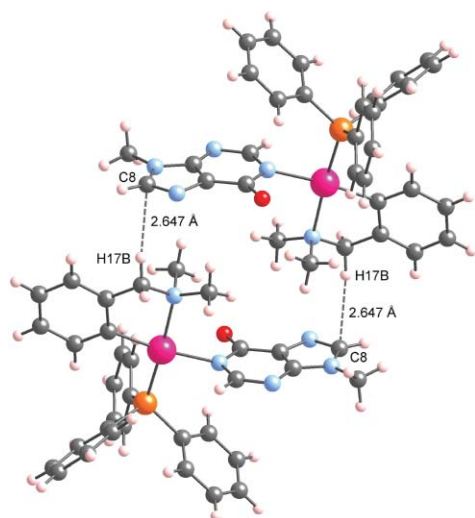


Fig. 5 Intermolecular C–H... π interactions in **6**.

upon basic treatment requires some detailed analysis. Assuming the limitations of the working level of theory, *e.g.* structures being optimized in the gas phase, in neutral medium the perchlorate counteranion acts as H-bond acceptor towards the amide-like NH group at position 1 of the ligand ($d_{\text{H}\cdots\text{O}} = 1.821 \text{ \AA}$), supplemented by a second weaker interaction ($d_{\text{H}\cdots\text{O}} = 2.244 \text{ \AA}$) (Fig. 6). This feature prevents the action of N1 as donor and increases slightly the electron density at N3 with respect to that in the parent neutral ligand 9-mhypH.²⁸ Pure electrostatic arguments based, for instance, on atomic natural charges²⁹ would lead to a wrong prediction, as N3 (-0.495 au) is expected to behave as more basic than N7 (-0.392 au). Mulliken charges vary similarly (-0.309 and -0.211 au for N3 and N7, respectively). Finally, steric crowding at N3, due to the proximity of the methyl substituent on N9, could be invoked in order to explain qualitatively the observed regioselectivity. In basic conditions the formal negative charge corresponding to the deprotonated ligand 9-mhypH⁻ is spread mainly on N3 ($q_{\text{N}} = -0.572 \text{ au}$) \geq N1 ($q_{\text{N}} = -0.545 \text{ au}$) \gg N7 ($q_{\text{N}} = -0.412 \text{ au}$). Owing to steric reasons N1 could be selected as the best donor candidate, in agreement with the experimental results.

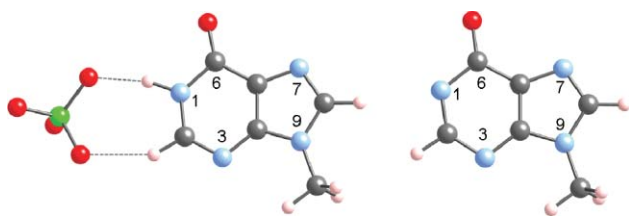


Fig. 6 Calculated (method B) structures for ligands 9-mhypH·ClO₄⁻ (left) and 9-mhyp⁻ (right).

The preference among several donor atoms to interact with an acidic centre can also be qualitatively analysed in the context of Pearson's hard–soft acid–base (HSAB) principle.³⁰ Besides the steric contribution that systematically unfavours binding through N3, the relatively soft Pt(II) centre will preferably interact with the softer donor centre, which is that with highest energy content for its basic electron lone pair. Using method C as the computation level, in 9-mhypH·ClO₄⁻ the uppermost MO containing nitrogen lone

pairs are HOMO-4 (HOMO has π symmetry, whereas HOMO-1, HOMO-2 and HOMO-3 are perchlorate-centered), HOMO-5 and HOMO-8 (Fig. 7a), all of them displaying higher quadratic coefficients³¹ on N7 than on N3 (0.021/0.008, 0.207/0.178 and 0.072/0.044, respectively). In the case of the anionic ligand 9-mhyp⁻ (Fig. 7b) HOMO-1 and HOMO-2 are mainly located on N1 (calculated coefficients ratio N1/N3/N7: 0.150/0.041/0.038 and 0.264/0.117/0.017, respectively), whereas in HOMO-4 the contribution of N7 (0.079/0.098/0.241) predominates and N3 only dominates in HOMO-6 (0.041/0.202/0.162). These relative sequences of MO are almost invariant as they are essentially kept on using other different types of hybrid exchange–correlation functionals such as LSDA.

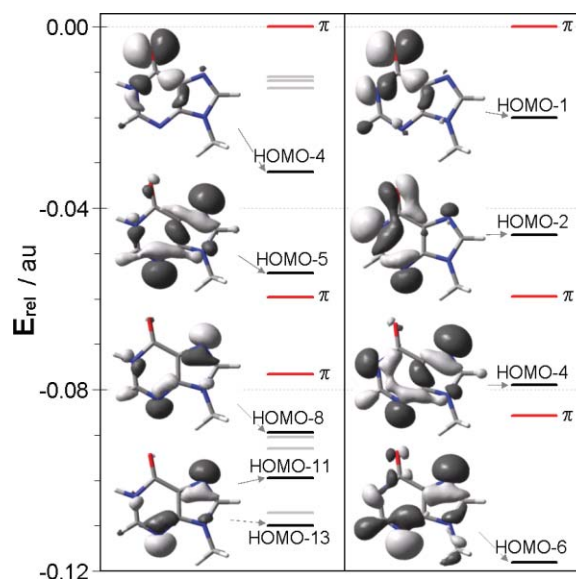


Fig. 7 Calculated (method C) MO diagram for (a) 9-mhypH·ClO₄⁻ (perchlorate anions omitted for clarity) and (b) 9-mhyp⁻. Energies (au) relative to the HOMO. Perchlorate-centered MO are displayed in gray.

Nevertheless, during the last two decades many important concepts and parameters related to chemical reactivity have been rationalized within the framework of DFT.³² The DFT formulation³³ of the HSAB principle states that the most favourable situation occurs when the reactants have equal softness, provided that the charge reshuffling step can be neglected. The best suited *local* reactivity index for studying regioselectivity³⁴ is local softness $s(\mathbf{r})$, easily obtained from the Fukui function $f(\mathbf{r})$, defined by Parr and Yang,³⁵ and the global softness $S = (\partial N / \partial \mu)_{v(\mathbf{r})}$, which describes the ability of the molecule to take or lose electrons in response to a change in the chemical potential, μ . Therefore $s(\mathbf{r})$ describes both the charge transfer between the reactants and how the charge is redistributed within the reactants themselves. A local HSAB principle can then be devised as follows: a regioisomer is favored when the new bond is formed between atoms of equal softness. In other words, the preferred regioisomer in the reaction between atom k in molecule A and molecule B will be formed on reaction at atom l that minimizes the quadratic difference in local condensed-to-atom softness function³⁶ $\Delta(s^2)_{kl} = (s_{Ak} - s_{Bl})^2$. For situations in which condensed local softness was found inadequate to provide the correct intermolecular reactivity trends, the group softness³⁷ descriptor, $s_{(k)g}$, has been highlighted, which is obtained after

Table 1 Relevant HSAB-related calculated (method B) parameters^a for the reaction of N-donor atoms in *L*H, *L*H·ClO₄⁻ and *L*⁻ with [Pt(dmba)(PPh₃)]⁺ and relative energies (method A) for the resulting products (*L*H = 9-mhypH)

| | | $\Delta(s^2)_{kl}^b$ | $\Delta\Omega_{kl}^c$ | E_{rel}^c |
|--|----|----------------------|-----------------------|-------------|
| <i>L</i> H | N3 | 0.58 | 3.8 | 55.9 |
| | N7 | 0.35 | 2.9 | 0.0 |
| <i>L</i> H·ClO ₄ ⁻ | N3 | 0.95 | 11.4 | 10.4 |
| | N7 | 0.71 | 6.7 | 0.0 |
| <i>L</i> ⁻ | N1 | 0.44 | 20.0 | 0.0 |
| | N3 | 0.55 | 29.5 | 67.6 |
| | N7 | 0.40 | 11.5 | 29.7 |

^a Derived from Mulliken charges. ^b Group property. ^c kJ mol⁻¹.

summing the condensed local softness over all of the *n* neighboring atoms attached to the reactive site *k*. Finally, in the very first step of the bond-forming interaction between atoms *k* and *l*, charge is transferred within them, equalizes the electron chemical potential and induces a variation of the grand potential $\Delta\Omega$ of the system. The contribution due to the interaction of atoms *k* and *l* is $\Delta\Omega_{kl} = -\frac{1}{2}(\mu_A - \mu_B)^2 s_{Ak} s_{Bl} / (s_{Ak} + s_{Bl})$. Table 1 collects the values for both parameters $\Delta(s^2)_{kl}$ and $\Delta\Omega_{kl}$ computed for the nucleophilic attack of all possible donor atoms in each case, 9-mhypH·ClO₄⁻ or 9-mhyp⁻ (the case of 9-mhypH is also included for comparison), to the Pt(II) centre in an hypothetical tricoordinated electrophilic [Pt(dmba)(PPh₃)]⁺ species³⁸ (Fig. 8).

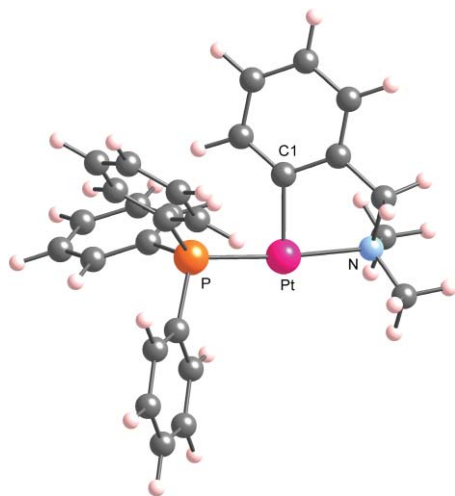


Fig. 8 Calculated (method B) structure (see text) for the electrophilic fragment [Pt(PPh₃)(dmba)]⁺.

For 9-mhypH·ClO₄⁻ the lowest interaction values—most favourable interactions—are observed for the imidazole-like N7 atom (the same holds for 9-mhypH) that, in addition, gives rise to the most stable product (Table 1). The large thermochemical instability arising from complexation through N3 in 9-mhypH, notably decreases in 9-mhypH·ClO₄⁻ due to intramolecular hydrogen bond formation. In the case of 9-mhyp⁻ a new donor atom N1 is now available. Here also the most unfavourable interaction (kinetic) parameters and most unstable (thermodynamic) complex formation corresponds to binding through N3. Nevertheless, discrimination between N1 and N7 is not properly predicted using HSAB-derived interaction parameters. On the contrary,

the complexation seems to be thermodynamically controlled as only the relative complex energy sequence agrees with the experimentally observed N1-complexation. This could tentatively point to a possible occurrence of such N1-coordination types in other not sterically hindered and relatively soft metal centres.

In spite of the fact that intermolecular interactions were not taken into account, at the highest level of theory (method B) both calculated structures [Pt(dmba)(PPh₃)](9-mhypH·ClO₄) and [Pt(dmba)(PPh₃)](9-mhyp) very nicely agree with those experimentally obtained by single-crystal X-ray diffraction analysis (see the ESI†).

Experimental

Instrumental measurements

The CHN analyses were performed with a Carlo Erba model EA 1108 microanalyzer. Decomposition temperatures were determined with a SDT 2960 simultaneous DSC-TGA from TA instruments at a heating rate of 5 °C min⁻¹ and the solid samples under nitrogen flow (100 mL min⁻¹). The ¹H and ³¹P NMR spectra were recorded on Bruker AC 300E, Bruker AC 400E or Bruker AV 600 spectrometers, using SiMe₄ and H₃PO₄ as standards. Infrared spectra were recorded on a Perkin-Elmer 1430 spectrophotometer using Nujol mulls between polyethylene sheets. All ESI spectra were recorded in positive mode and performed on a LC-MS Agilent VL system.

Materials

The starting complexes [M(dmba)Cl(L)] (M = Pd or Pt; L = PPh₃, PTA or DMSO),^{15,16} and [Pd(dmba)(μ-OH)]₂,²⁶ were prepared by procedures described elsewhere. Solvents were dried by the usual methods.

Warning! Perchlorate salts of metal complexes with organic ligands are potentially explosive. Only small amounts of material should be prepared, and these should be handled with great caution.

Preparation of complexes

[M(dmba)(PPh₃)(9-mhypH)]ClO₄ [M = Pd (1), Pt (2)]. To a solution of [M(dmba)(Cl)(PPh₃)] (0.185 mmol) in CH₂Cl₂ (20 ml) was added AgClO₄ (38.4 mg, 0.185 mmol). AgCl immediately formed. The resulting suspension was stirred for 1 h and then filtered through a short pad of Celite®. To the filtrate was then added 9-mhypH (27.8 mg, 0.185 mmol). The solution was stirred for 5 h (complex 1) or 20 h (complex 2), and then the solvent was partially evaporated under vacuum and hexane added to precipitate a white solid, which was collected by filtration and air-dried. **1:** Yield: 94 mg (68%). Calcd. for C₃₃H₃₃ClN₅O₃PPd: C 52.7, H 4.4, N 9.3. Found: C 52.3, H, 4.5, N 9.0. Mp: 201 °C (dec). IR (Nujol, cm⁻¹): 3180 ν(NH); 1704 ν(CO); ClO₄, 1094, 622. ¹H NMR (CDCl₃): δ 10.26 (s, 1H, NH of 9-mhypH), 8.08 (s, 1H, H8 of 9-mhypH), 7.95 (s, 1H, H2 of 9-mhypH), 7.61 (m, 6H, PPh₃), 7.28 (m, 9H, PPh₃), 6.97 (d, 1H, C₆H₄, J_{HH} = 6.9 Hz), 6.82 (m, 1H, C₆H₄), 6.34 (m, 2H, C₆H₄), 4.22 (brm, 1H, NCH₂ of dmba), 4.00 (brm, 1H, NCH₂ of dmba), 3.60 (brs, 3H, Me of 9-mhypH), 2.64 (brs, 3H, NMe₂ of dmba), 2.52 (brs, 3H,

NMe_2 of dmbs). ^{31}P NMR ($CDCl_3$): $\delta(H_3PO_4)$ 42.6 (s). ESI⁺ mass spectra (CH_3CN): m/z +651.8 ([Pd(dmbs)(PPh₃)(9-mhypH)]⁺ -1, 12%); +501.3 ([Pd(dmbs)(PPh₃)]⁺ -2, 100%). **2**: Yield: 132 mg (85%). Calcd. for $C_{33}H_{33}ClN_5O_5PPt$: C 47.1, H 4.0, N 8.3. Found: C 47.2, H, 4.1, N 8.5. Mp: 292 °C (dec). IR (Nujol, cm^{-1}): 3188 $\nu(NH)$; 1708 $\nu(CO)$; ClO_4 , 1100, 624. 1H NMR ($CDCl_3$): δ 10.48 (s, 1H, NH of 9-mhypH), 8.06 (s, 1H, H8 of 9-mhypH), 7.95 (s, 1H, H2 of 9-mhypH), 7.64 (m, 6H, PPh₃, Pt satellites are observed as shoulders), 7.20 (m, 9H, PPh₃), 7.01 (d, 1H, C_6H_4 , $J_{HH} = 6.9$ Hz), 6.83 (m, 1H, aromatic of dmbs), 6.40 (dd, 1H, $J_{HH} = 7.3$ Hz, $J_{HP} = 2.4$ Hz, aromatic of dmbs, Pt satellites are observed as shoulders), 6.35 (m, 2H, aromatic of dmbs), 4.19 (dd, 1H, NCH_2 of dmbs, $J_{HH} = 13.0$ Hz, $J_{HP} = 1.5$ Hz, Pt satellites are observed as shoulders), 4.05 (dd, 1H, NCH_2 of dmbs, $J_{HH} = 13.0$ Hz, $J_{HP} = 2.8$ Hz, Pt satellites are observed as shoulders), 3.63 (s, 3H, Me of 9-mhypH), 2.75 (d, 3H, NMe_2 of dmbs, $J_{HP} = 2.4$ Hz, Pt satellites are observed as shoulders), 2.66 (d, 3H, NMe_2 of dmbs, $J_{HP} = 2.7$ Hz, Pt satellites are observed as shoulders). ^{31}P NMR ($CDCl_3$): $\delta(H_3PO_4)$ 20.3 (s, $J_{PPT} = 4171$ Hz). ESI⁺ mass spectra (CH_3CN): m/z +740.9 ([Pt(dmbs)(PPh₃)(9-mhypH)]⁺, 100%), +591.1 ([Pt(dmbs)(PPh₃)]⁺, 61%).

Preparation of complex

[Pt(dmbs)(DMSO)(9-mhypH)ClO₄] (3). To a solution of [Pt(dmbs)(Cl)(DMSO)] (100 mg, 0.226 mmol) in acetone (20 ml) was added $AgClO_4$ (46.9 mg, 0.226 mmol). $AgCl$ immediately formed. The resulting suspension was stirred for 1 h and then filtered through a short pad of Celite®. To the filtrate was then added 9-mhypH (33.9 mg, 0.226 mmol). The solution was stirred for 20 h, and then the solvent was concentrated to dryness under reduced pressure. Addition of ether yielded a white solid, which was collected by filtration and air-dried. Yield: 117 mg (79%). Calcd. for $C_{17}H_{24}ClN_5O_6SPt$: C 31.1, H 3.7, N 10.7, S, 4.9. Found: C 31.2, H, 3.5, N 10.4, S, 5.0. Mp: 257 °C (dec). IR (Nujol, cm^{-1}): 3180 $\nu(NH)$; 1704 $\nu(CO)$; ClO_4 , 1096, 624. 1H NMR ($DMF-d_7$): δ 13.03 (brs, 2H, NH of 9-mhypH), 9.17 (s, 2H, H8 of 9-mhypH), 8.48 (1H, H2 of 9-mhypH), 8.47 (1H, H2 of 9-mhypH), 7.86 (m, 2H, C_6H_4), 7.17 (d, 2H, aromatic of dmbs, $J_{HH} = 7.2$ Hz), 7.09 (m, 2H, aromatic of dmbs, Pt satellites are observed as shoulders), 7.02 (m, 2H, aromatic of dmbs), 4.22 (d, 2H, NCH_2 of dmbs, $J_{HH} = 14.0$ Hz, Pt satellites are observed as shoulders), 4.05 (d, 2H, NCH_2 of dmbs, $J_{HH} = 14.0$ Hz), 4.01 (s, 6H, Me of 9-mhypH), 3.35 (s, 6H, DMSO, Pt satellites are observed as shoulders), 3.11 (s, 6H, DMSO, $J_{HH} = 53.8$ Hz), 2.63 (s, 6H, NMe_2 of dmbs, Pt satellites are observed as shoulders), 2.48 (s, 6H, NMe_2 of dmbs). ESI⁺ mass spectra (CH_3CN): m/z +556.9 ([Pt(dmbs)(DMSO)(9-mhypH)]⁺, 12%); +406.5.1 ([Pt(dmbs)(DMSO)]⁺, 100%).

Preparation of complex

[Pt(dmbs)(PTA)(9-mhypH)ClO₄] (4). To a solution of [Pt(dmbs)(Cl)(PTA)] (100 mg, 0.192 mmol) in acetone (20 ml) was added $AgClO_4$ (39.7 mg, 0.192 mmol). $AgCl$ immediately formed. The resulting suspension was stirred for 1 h and then filtered through a short pad of Celite®. To the filtrate was then added 9-mhypH (28.76 mg, 0.191 mmol). After stirring at room temperature for 20 h a small amount of white solid was removed by filtration. The filtrate was concentrated under vacuum affording

crystals of complex **4**, which were collected by filtration and air-dried. Yield: 99 mg (70%). Calcd. for $C_{21}H_{30}ClN_8O_5PPt$: C 34.3, H 4.1, N 15.2. Found: C 34.8, H, 4.1, N 16.4. Mp: 262 °C (dec). IR (Nujol, cm^{-1}): 3147 $\nu(NH)$; 1700 $\nu(CO)$; ClO_4 , 1097, 623. 1H NMR ($DMF-d_7$): δ 12.91 (s, 2H, NH of 9-mhypH), 8.94 (s, 2H, H8 of 9-mhypH), 8.46 (s, H, H2 of 9-mhypH), 8.45 (s, H, H2 of 9-mhypH), 7.60 (m, 2H, C_6H_4 , Pt satellites are observed as shoulders), 7.15 (m, 2H, C_6H_4), 7.04 (m, 4H, C_6H_4), 4.54 (d, 6H, NCH_2N of PTA, $J_{HH} = 12.8$ Hz), 4.46 (d, 6H, NCH_2N of PTA, $J_{HH} = 12.8$ Hz), 4.20 (d, 6H, NCH_2P of PTA, $J_{HH} = 15.9$ Hz), 4.12 (d, 6H, NCH_2P of PTA, $J_{HH} = 15.9$ Hz), 4.02 (d, 4H, NCH_2 of dmbs, $J_{HP} = 2.6$ Hz), 4.00 (s, 6H, Me of 9-mhypH), 2.50 (d, 6H, NMe_2 of dmbs, $J_{HP} = 2.6$ Hz, Pt satellites are observed as shoulders), 2.45 (d, 6H, NMe_2 of dmbs, $J_{HP} = 2.6$ Hz, Pt satellites are observed as shoulders). ^{31}P NMR ($DMF-d_7$): $\delta(H_3PO_4)$ -64.87 (s, $J_{PPT} = 3669$ Hz). ESI⁺ mass spectra (CH_3CN): m/z +635.8 ([Pt(dmbs)(PTA)(9-mhypH)]⁺, 100%); +485.7 ([Pt(dmbs)(PTA)]⁺, 45%).

Preparation of complex [Pd(dmbs)(PPh₃)(9-mhyp)] (5). To a solution of [Pd(dmbs)(μ -OH)]₂ (100 mg, 0.195 mmol) in CH_2Cl_2 (20 ml) was added PPh_3 (102.4 mg, 0.390 mmol) and 9-mhypH (58.61 mg, 0.390 mmol). The solution was stirred for 6 h at room temperature, and then the solvent was concentrated to dryness under reduced pressure. Addition of ether yielded a white solid, which was collected by filtration and air-dried. Yield: 201 mg (79%). Calcd. for $C_{33}H_{32}N_5OPPd$: C 60.8, H 5.0, N 10.7. Found: C 60.7, H, 5.0, N 10.5. Mp: 241 °C (dec). IR (Nujol, cm^{-1}): 1632 $\nu(CO)$. 1H NMR ($CDCl_3$) at 0 °C: δ 7.68 (m, 6H, PPh₃), 7.63 (s, 1H, H2 of 9-mhypH), 7.44 (s, 1H, H8 of 9-mhypH), 7.24 (m, 9H, PPh₃), 7.03 (d, 1H, C_6H_4 , $J_{HH} = 7.2$ Hz), 6.86 (m, 1H, C_6H_4), 6.40 (m, 2H, C_6H_4), 4.23 (d, 1H, NCH_2 of dmbs, $J_{HH} = 12.9$ Hz), 3.99 (dd, 1H, NCH_2 of dmbs, $J_{HH} = 12.9$ Hz, $J_{HP} = 2.4$ Hz), 3.58 (s, 3H, Me of 9-mhypH), 2.80 (brs, 3H, NMe_2 of dmbs), 2.56 (brs, 3H, NMe_2 of dmbs). ^{31}P NMR ($CDCl_3$): $\delta(H_3PO_4)$ 43.4 (s). ESI⁺ mass spectra (CH_3CN): m/z +652.1 ([Pd(dmbs)(PTA)(9-mhypH)]⁺, 5%); +502.4 ([Pd(dmbs)(PTA)]⁺, 47%).

Preparation of complexes

[Pt(dmbs)(L)(9-mhyp)] [L = PPh₃ (6), PTA (7)]. To a solution of [Pt(dmbs)(Cl)(L)] (0.159 mmol) in acetone (20 ml) was added $AgClO_4$ (33.0 mg, 0.159 mmol). $AgCl$ immediately formed. The resulting suspension was stirred for 1 h and then filtered through a short pad of Celite®. To the filtrate was then added a solution containing 20% $[NBu_4]OH(aq)$ (208 μ L, 0.159 mmol) and 9-mhypH (23.9 mg, 0.159 mmol). After stirring at room temperature for 10 h, the solvent was partially eliminated under reduced pressure to yield a white precipitate. The solid was collected by filtration and air-dried. **6**: Yield: 93 mg (75%). Calcd. for $C_{33}H_{32}N_5OPPt$: C 53.5, H 4.4, N 9.5. Found: C 53.6, H, 4.4, N 9.2. Mp: 320 °C (dec). IR (Nujol, cm^{-1}): 1634 $\nu(CO)$. 1H NMR ($DMF-d_7$) at room temperature: δ 7.71 (m, 6H, PPh₃), 7.70 (s, 1H, H2 of 9-mhyp), 7.42 (s, 1H, H8 of 9-mhyp), 7.21 (m, 9H, PPh₃), 7.04 (d, 1H, C_6H_4 , $J_{HH} = 7.4$ Hz), 6.85 (m, 1H, aromatic of dmbs), 6.51 (dd, 1H, $J_{HH} = 7.4$ Hz, $J_{HP} = 2.5$ Hz, aromatic of dmbs), 6.39 (m, 1H, aromatic of dmbs), 4.23 (d, 1H, NCH_2 of dmbs, $J_{HH} = 13.4$ Hz), 3.96 (dd, 1H, NCH_2 of dmbs, $J_{HH} = 13.4$ Hz, $J_{HP} = 3.6$ Hz, Pt satellites are observed as shoulders), 3.56 (s, 3H, Me of 9-mhyp), 2.94 (d, 3H, NMe_2 of dmbs, $J_{HP} = 2.4$ Hz), 2.64 (d, 3H, NMe_2 of dmbs, $J_{HP} = 2.6$ Hz). ^{31}P NMR

(DMF- d_7): $\delta(\text{H}_3\text{PO}_4)$ 20.8 (s, $J_{\text{Ppt}} = 4279$ Hz). ESI⁺ mass spectra (CH₃CN): $m/z + 740.2$ ([Pt(dmba)(PPh₃)(9-mhyp)]⁺, 22%); $+591.4$ ([Pt(dmba)(PPh₃)]⁺ + 1, 100%). **7**: Yield: 76 mg (65%). Calcd. for C₂₁H₂₉N₄₈OPPt: C 39.7, H 4.6, N 17.6. Found: C 39.4, H, 4.8, N 17.8. Mp: 305 °C (dec). IR (Nujol, cm⁻¹): 1632 $\nu(\text{CO})$. ¹H NMR (DMF- d_7) at room temperature: δ 8.13 (s, 1H, H2 of 9-mhyp), 7.91 (s, 1H, H8 of 9-mhyp), 7.60 (m, 1H, C₆H₄, Pt satellites are observed as shoulders), 7.16 (m, 1H, C₆H₄), 7.00 (m, 2H, C₆H₄ Pt satellites are observed as shoulders), 4.58 (d, 3H, NCH₂N of PTA, $J_{\text{HH}} = 12.9$ Hz), 4.48 (d, 3H, NCH₂N of PTA, $J_{\text{HH}} = 12.9$ Hz), 4.24 (d, 3H, NCH₂P of PTA, $J_{\text{HH}} = 15$ Hz), 4.19 (d, 3H, NCH₂P of PTA, $J_{\text{HH}} = 15$ Hz), 4.12 (d, 2H, NCH₂ of dmba, $J_{\text{HH}} = 13.7$ Hz), 3.94 (dd, 2H, NCH₂ of dmba, $J_{\text{HH}} = 13.7$ Hz, $J_{\text{HP}} = 3.3$ Hz), 3.79 (s, 3H, Me of 9-mhyp), 2.61 (d, 3H, NMe₂ of dmba, $J_{\text{HP}} = 1.9$ Hz), 2.53 (d, 3H, NMe₂ of dmba, $J_{\text{HP}} = 2.4$ Hz, $J_{\text{HPt}} = 37.5$ Hz). ³¹P NMR (DMF- d_7): $\delta(\text{H}_3\text{PO}_4) -64.8$ (s, $J_{\text{Ppt}} = 3802$ Hz). ESI⁺ mass spectra (CH₃CN): $m/z + 636.2$ ([Pt(dmba)(PTA)(9-mhyp)]⁺ + 1, 12%); $+486.4$ ([Pt(dmba)(PTA)]⁺ + 1, 10%).

X-Ray crystal structure analysis

Suitable crystals from **2** and **6** were grown from dichloromethane/hexane. The crystal and molecular structures of the compounds **2** and **6** have been determined by X-ray diffraction studies (Table 2). Compounds **2** and **6** were measured on a Bruker Smart Apex diffractometer. Data were collected using

Table 2 Crystal structure determination details

| Compound | 2 | 6 |
|---|---|---|
| Empirical formula | C ₃₃ H ₃₃ ClN ₅ O ₅ PPt | C ₃₃ H ₃₃ N ₅ OPPt |
| fw (g mol ⁻¹) | 841.15 | 740.70 |
| Cryst system | triclinic | triclinic |
| <i>a</i> (Å) | 8.8061(4) | 8.4884(4) |
| <i>b</i> (Å) | 9.5922(5) | 10.0705(5) |
| <i>c</i> (Å) | 19.6841(11) | 17.4286(8) |
| α (deg) | 94.609(2) | 103.460(2) |
| β (deg) | 100.862(2) | 94.548(2) |
| γ (deg) | 102.408(2) | 90.602(2) |
| <i>V</i> (Å ³) | 1582.07(14) | 4653.8(4) |
| Temp (K) | 100(2) | 100(2) |
| Space group | <i>P</i> -1 | <i>P</i> -1 |
| <i>Z</i> | 2 | 2 |
| <i>D</i> _{calc} (Mg m ⁻³) | 1.766 | 1.704 |
| μ (mm ⁻¹) | 4.620 | 4.951 |
| <i>F</i> (000) | 832 | 732 |
| Crystal size (mm) | 0.31 × 0.24 × 0.17 | 0.13 × 0.07 × 0.05 |
| 2 θ range (°) | 2.12–26.37 | 2.08–27.09 |
| <i>h</i> ; <i>k</i> ; <i>l</i> (range) | –10 ≤ <i>h</i> ≤ 10 –11 ≤ <i>k</i> ≤ 11 –24 ≤ <i>l</i> ≤ 24 | –10 ≤ <i>h</i> ≤ 10 –12 ≤ <i>k</i> ≤ 12 –22 ≤ <i>l</i> ≤ 21 |
| Max./min. transmission | 0.5072/0.3285 | 0.6888/0.4884 |
| Reflect. collcd [<i>I</i> > 2 σ (<i>I</i>)] | 17320 | 16441 |
| Independent reflections | 6396 | 6233 |
| <i>R</i> (int) | 0.0140 | 0.0281 |
| Restraints/parameters | 0/422 | 0/373 |
| Goodness-of-fit on <i>F</i> ² ^a | 1.083 | 1.098 |
| <i>R</i> ₁ / <i>wR</i> ₂ [<i>I</i> > 2 σ (<i>I</i>)] ^b | 0.0158/0.0392 | 0.0280/0.0620 |
| <i>R</i> ₁ / <i>wR</i> ₂ (all reflect.) ^c | 0.0162/0.0394 | 0.0301/0.628 |
| Max./min. $\Delta\rho^d/e$ Å ⁻³ | 0.873/-0.793 | 1.625/-1.565 |

^a Goodness-of-fit = $[\sum[w(F_o^2 - F_c^2)^2]/(n - p)]^{1/2}$; ^b $R_1 = \sum|F_o| - |F_c|/\sum|F_o|$, $wR_2 = [\sum[w(F_o^2 - F_c^2)^2]/\sum w(F_o^2)^2]^{1/2}$; ^c $w = 1/[\sigma^2(F_o^2) + (aP)^2 + bP]$, where $P = (2F_o^2 + F_c^2)/3$ and *a* and *b* are constants set by the program; ^d Largest difference peak and hole.

monochromated Mo K α radiation in ω scan mode. Absorption corrections were applied on the basis of multi-scans. All structures were solved by direct methods using SHELX-97³⁹ and refined anisotropically on *F*². The NH hydrogen atoms were found and refined with $U_{\text{iso}}(\text{H}) = 1.2U_{\text{eq}}(\text{N})$. Hydrogen atoms for aromatic CH, aliphatic CH, CH₂ and methyl groups were positioned geometrically (C–H = 0.98 Å for CH₂, C–H = 0.97 Å for CH₃) and refined using a riding model (AFIX 43 for aromatic CH, AFIX 13 for aliphatic CH, AFIX 23 for CH₂, AFIX 137 for CH₃), with $U_{\text{iso}}(\text{H}) = 1.2U_{\text{eq}}(\text{CH}, \text{CH}_2)$ and $U_{\text{iso}}(\text{H}) = 1.5U_{\text{eq}}(\text{CH}_3)$.

Computational details

The reliably accurate description of weak interactions like those between ligands and heavy metals generally requires a treatment of electron correlation. Density functional theory (DFT)⁴⁰ has proved quite useful in this regard offering an electron correlation correction frequently comparable to the second-order Møller–Plesset theory (MP2) or in certain cases, and for certain purposes, even superior to MP2, but at considerably lower computational cost.⁴¹ Calculated geometries at the DFT level were fully optimized in the gas-phase with tight convergence criteria using the Gaussian 03 package,⁴² employing the BP86 functional. The 6-31G** basis set was used in the optimizations for all atoms and adding diffuse functions on N, O and P atoms (denoted as aug6-31G**), as well as the Stuttgart relativistic small-core basis set with effective core potential (StRSCecp) for Pt (method A). Thereafter only the most stable complexes as well as the individual formal components 9-mhypH, 9-mhypH·ClO₄⁻, 9-mhyp⁻ and [Pt(PPh₃)(dmba)]⁺ were refined using the same functional and the most extensive def2TZVP basis set for all atoms, with effective core potential for Pt (method B), that was used as the standard level of theory unless otherwise stated. From these gas-phase optimized geometries all reported data were obtained by means of single-point (SP) calculations at the same level. Energy values are uncorrected for the zero-point vibrational energy. Natural charges were obtained from the Natural Bond Orbital (NBO) population analysis. The MO isosurfaces and energies displayed in Fig. 7 were computed at the B3LYP/def2TZVP level (method C).

Acknowledgements

This work was supported by the Ministerio de Educacion y Ciencia of Spain and FEDER (Project CTQ2008-02178/BQU) and Fundación Séneca-CARM (Project 08666/PI/08). A.E. would like to acknowledge financial support from MICINN-Spain, Project CTQ2008-01402 and Fundación Séneca (Project 04509/GERM/06).

Notes and references

- 1 For a comprehensive collection of review articles, see: *Cisplatin–Chemistry and Biochemistry of a Leading Anticancer Drug*, ed. B. Lippert, Wiley-VCH, Zürich, 1999.
- 2 J. Reedijk, *Proc. Natl. Acad. Sci. U. S. A.*, 2003, **100**, 3611.
- 3 K. D. Klika and J. Arpalahiti, *Chem. Commun.*, 2004, 666.
- 4 B. Lippert, *Coord. Chem. Rev.*, 2000, **200–202**, 487–516, and references cited therein.
- 5 H. Chen, J. A. Parkinson, R. E. Morris and P. J. Sadler, *J. Am. Chem. Soc.*, 2003, **125**, 173–186.
- 6 B. Longato, D. Montagner and E. Zangrando, *Inorg. Chem.*, 2006, **45**, 8179–8187.

- 7 J. Ruiz, N. Cutillas, C. Vicente, M. D. Villa, G. López, J. Lorenzo, F. X. Avilés, V. Moreno and D. Bautista, *Inorg. Chem.*, 2005, **44**, 7365–7376.
- 8 J. Ruiz, M. D. Villa, V. Rodríguez, N. Cutillas, C. Vicente, G. López and D. Bautista, *Inorg. Chem.*, 2007, **46**, 5448–5449.
- 9 J. Ruiz, M. D. Villa, N. Cutillas, G. López, D. Bautista, V. Moreno and L. Valencia, *Inorg. Chem.*, 2008, **47**, 4490–4505.
- 10 A. Moe, J. Ringvoll, L. M. Nordstrand, L. Eide, M. Bjoras, E. Seeberg, T. Rognes and A. Klungland, *Nucleic Acids Res.*, 2003, **31**, 3893; D. L. Foss, M. J. Baarsch and M. P. Murtaugh, *Anim. Biotechnol.*, 1998, **9**, 67.
- 11 J. Arpalahiti and K. D. Klika, *Eur. J. Inorg. Chem.*, 2003, (23), 4195–4201.
- 12 P. J. Sanz Miguel and B. Lippert, *Dalton Trans.*, 2005, (9), 1679–1686.
- 13 E. Freisinger, I. B. Rother, M. S. Lüth and B. Lippert, *Proc. Natl. Acad. Sci. U. S. A.*, 2003, **100**, 3748–3753.
- 14 CCDC CSD version 5.30, November 2008 + 3 updates.
- 15 A. J. Deeming, I. P. Rothwell, M. B. Hursthouse and L. New, *J. Chem. Soc., Dalton Trans.*, 1978, 1490–1496.
- 16 M. D. Meijer, A. W. Kleij, B. S. Williams, D. Ellis, M. Lutz, A. L. Spek, G. P. M. van Klink and G. van Koten, *Organometallics*, 2002, **21**, 264–271.
- 17 W. J. Geary, *Coord. Chem. Rev.*, 1971, **7**, 81–122.
- 18 K. Nakamoto, *Infrared and Raman Spectra of Inorganic and Coordination Compounds*, 5th ed.; Wiley-Interscience, New York, 1997, p 199.
- 19 J. Ruiz, V. Rodríguez, N. Cutillas, G. López and D. Bautista, *Inorg. Chem.*, 2008, **47**, 10025–10036.
- 20 S. Otto, P. V. Samuleev, V. A. Polyakov, A. D. Ryabov and L. I. Elding, *Dalton Trans.*, 2004, 3662–3668.
- 21 J. Ruiz, N. Cutillas, F. López, G. López and D. Bautista, *Organometallics*, 2006, **25**, 5768–5773.
- 22 C. Janiak, *J. Chem. Soc., Dalton Trans.*, 2000, 3885–3896.
- 23 F. Babudri, G. M. Farinola, F. Naso and R. Ragni, *Chem. Commun.*, 2007, 1003–1022.
- 24 M. Nishio, *CrystEngComm*, 2004, **6**(27), 130–158.
- 25 J. Ruiz, J. Lorenzo, C. Vicente, G. López, J. M. López-De-Luzuriaga, M. Monge, F. X. Avilés, D. Bautista, V. Moreno and A. Laguna, *Inorg. Chem.*, 2008, **47**, 6990–7001.
- 26 J. Ruiz, N. Cutillas, V. Rodríguez, J. Sampedro, G. López, P. A. Chaloner and P. B. Hitchcock, *J. Chem. Soc., Dalton Trans.*, 1999, 2939–2946.
- 27 J. Arpalahiti, E. Niskanen and R. Sillanpää, *Chem.–Eur. J.*, 1999, **5**, 2306–2311.
- 28 Variation of natural charges on N3 and N7 $\Delta q_N = -0.036$ and -0.016 e, respectively.
- 29 (a) J. E. Carpenter and F. Weinhold, *J. Mol. Struct. (Theochem)*, 1988, **169**, 41–62; (b) J. E. Carpenter, Ph.D. thesis, University of Wisconsin, Madison, WI, 1987; (c) J. P. Foster and F. Weinhold, *J. Am. Chem. Soc.*, 1980, **102**, 7211–7218; (d) A. E. Reed and F. Weinhold, *J. Chem. Phys.*, 1983, **78**, 4066–4073; (e) A. E. Reed, R. B. Weinstock and F. Weinhold, *J. Chem. Phys.*, 1985, **83**, 735–746; (f) A. E. Reed, L. A. Curtiss and F. Weinhold, *Chem. Rev.*, 1988, **88**, 899–926.
- 30 R. G. Pearson, *J. Am. Chem. Soc.*, 1963, **85**, 3533–3539.
- 31 Calculated as the sum of the squared coefficients of all AO contributing at that atom.
- 32 R. G. Parr and W. Yang, *Density Functional Theory of Atoms and Molecules*, Oxford University Press, Oxford, 1989.
- 33 (a) P. K. Chattaraj, H. Lee and R. G. Parr, *J. Am. Chem. Soc.*, 1991, **113**, 1855–1856; (b) A. Cedillo, P. K. Chattaraj and R. G. Parr, *Int. J. Quantum Chem.*, 2000, **77**, 403–407.
- 34 See for instance: A. Ponti and G. Molteni, *Chem.–Eur. J.*, 2006, **12**, 1156–1161 and references cited therein.
- 35 R. G. Parr and W. Yang, *J. Am. Chem. Soc.*, 1984, **106**, 4049–4050.
- 36 (a) S. Damoun, G. Van deWoude, F. Méndez and P. Geerlings, *J. Chem. Phys.*, 1997, **101**, 886–893; (b) A. Ponti, *J. Phys. Chem. A*, 2000, **104**, 8843–8846.
- 37 F. De Proft, W. Langenaeker and P. Geerlings, *J. Phys. Chem.*, 1993, **97**, 1826–1831; F. De Proft, S. Amira, K. Choho and P. Geerlings, *J. Phys. Chem.*, 1994, **98**, 5227–5233; S. Krishnamurty and S. Pal, *J. Phys. Chem. A*, 2000, **104**, 7639–7645.
- 38 The species $[\text{Pt}(\text{dmba})(\text{PPh}_3)]^+$ has been obtained by constrained optimization keeping the dihedral N–C1–Pt–P at 180° and an orthogonal C1–Pt–P angle.
- 39 G. M. Sheldrick, *SHELXS-97, SHELXL-97, Programs for Crystal Structure Analysis*, University of Göttingen, Germany, 1997.
- 40 L. J. Bartolotti and K. Fluchick, in *Reviews in Computational Chemistry*, ed. K. B. Lipkowitz and B. D. Boyd, VCH, New York, 1996, vol. 7, pp. 187–216.
- 41 P. R. Rablen, J. W. Lockman and W. L. Jorgensen, *J. Phys. Chem. A*, 1998, **102**, 3782–3797.
- 42 M. J. Frisch, G. W. Trucks, H. B. Schlegel, G. E. Scuseria, M. A. Robb, J. R. Cheeseman, J. A. Montgomery, Jr., T. Vreven, K. N. Kudin, J. C. Burant, J. M. Millam, S. S. Iyengar, J. Tomasi, V. Barone, B. Mennucci, M. Cossi, G. Scalmani, N. Rega, G. A. Petersson, H. Nakatsuji, M. Hada, M. Ehara, K. Toyota, R. Fukuda, J. Hasegawa, M. Ishida, T. Nakajima, Y. Honda, O. Kitao, H. Nakai, M. Klene, X. Li, J. E. Knox, H. P. Hratchian, J. B. Cross, V. Bakken, C. Adamo, J. Jaramillo, R. Gomperts, R. E. Stratmann, O. Yazyev, A. J. Austin, R. Cammi, C. Pomelli, J. Ochterski, P. Y. Ayala, K. Morokuma, G. A. Voth, P. Salvador, J. J. Dannenberg, V. G. Zakrzewski, S. Dapprich, A. D. Daniels, M. C. Strain, O. Farkas, D. K. Malick, A. D. Rabuck, K. Raghavachari, J. B. Foresman, J. V. Ortiz, Q. Cui, A. G. Baboul, S. Clifford, J. Cioslowski, B. B. Stefanov, G. Liu, A. Liashenko, P. Piskorz, I. Komaromi, R. L. Martin, D. J. Fox, T. Keith, M. A. Al-Laham, C. Y. Peng, A. Nanayakkara, M. Challacombe, P. M. W. Gill, B. G. Johnson, W. Chen, M. W. Wong, C. Gonzalez and J. A. Pople, *GAUSSIAN 03 (Revision B.2)*, Gaussian, Inc., Wallingford, CT, 2004.